Bulgarian Chemical Communications, Volume 48, Number 2 (pp. 297 – 302) 2016

Studying the effect of doping metal ions onto a crystalline hematite-based humidity sensor for environmental control

A. S. Afify[1*], M. Ataalla[2], A. Hussain[1], M. Hassan[1], A. Mohammed[3], M. Milanova[4], J.M. Tulliani[1]

[1] *Politecnico di Torino, Department of Applied Science and Technology, 10129 Torino, Italy*
[2] *University of Chemical Technology and Metallurgy, Department of Materials Science, 1756 Sofia, Bulgaria*
[3] *Chemistry Department, Deanery of Academic Services, Taibah University, Al-Madinah Al-Munawwarah, Saudi Arabia. On vacation from the Higher Institute of Optics Technology, Heliopolis, Cairo, Egypt*
[4] *Institute of General and Inorganic Chemistry, BAS, Acad. G. Bonchev Str. bld. 11, 1113 Sofia, Bulgaria*

Received March 24, 2015, Revised October 26, 2015

Humidity sensors have several applications in both industrial processing and environmental control. Pure and doped hematite has proved to exhibit remarkable humidity sensing properties. The aim of this investigation is to study the effect of doping of some metal ions (Li^{+},Mg^{+2}, Ba^{+2}, Sr^{+2}, and Na^{+}) onto the crystalline hematite and to determine their sensitivity towards relative humidity (RH). The obtained crystalline samples were characterized by X-Ray Diffraction (XRD) combined with Field Emission Scanning Electron Microscopy (FESEM). The doped sodium metal ions (Na^{+}) hematite sample showed a significant response towards relative humidity at room temperature.

Keywords: Doping, Hematite, Humidity sensors.

INTRODUCTION

Measurements and/or control of humidity are important not only for human comfort but also for a broad spectrum of industries and technologies. Humidity sensors have several applications in industrial processing, domestic applications and environmental control [1-4].

Adding metal ions to humidity sensing materials have been widely reported in literature due to their abundance in nature hence, efforts were made to denote their effects [5]. Doping of metal ions affects the microstructure and creates surface defects or oxygen vacancies of the sensing material [6-8].

Ferric oxide has a wide range of applications as a magnetic material [9]. In addition it is very sensitive to humidity and can be used as a humidity sensor [10]. α-Fe_2O_3 is an n-type semiconductor, it is the most stable iron oxide under ambient conditions, nontoxic, corrosion-resistant, low cost and abundant. These features render it suitable for numerous promising applications, such as catalysts/photocatalysts [11-13], contrast reagents/drug delivery [14] and gas sensors [15].

Nanocomposite materials containing α-Fe_2O_3 doped with noble metals (e.g., Pd, Pt, and Au) can lead to a synergetic effect depending on the preparation conditions, chemical composition, sintering temperature, sintering time and doping with various additives [16]. Different techniques were used for producing hematite films on the solid substrate like sputtering [17], laser ablation[18], electrodeposition [19], spray pyrolysis (SP) [20, 21], ion beam induced chemical vapor deposition (IBICVD) [22], plasma enhanced chemical vapor deposition (PECVD) [23] and aerosol- assisted chemical vapor deposition (AACVD) [24]. The aim of this study is to investigate the doping effect of some metal ions (Mg^{+2}, Ba^{+2}, Sr^{+2}, Li^{+}, and Na^{+}) onto a crystalline hematite and to determine their sensitivity to humidity. The sensors studied were prepared by a screen printing technique.

EXPERIMENTAL

Powder synthesis

All reagents were ACS grade from Sigma-Aldrich. 1 mole of α-Fe_2O_3 powder (Aldrich >99%, particle size distribution lower than 2 μm) was dispersed in distilled water, then a dispersing agent was added (Daraven 2 wt% of the used powder).
The solution was then ultrasonicated for 2 h. The prepared dispersed solution was mixed stepwise with 1.0 L aqueous solution of the salts (for precipitation of metal hydroxide as the pH was adjusted with NaOH): Li_2CO_3, $MgCO_3$, $Ba(NO_3)_2$, $Sr(No_3)_2$ and Na_2CO_3.

The dispersed solution was ultrasonicated again for 1 h, the solid content in solution was diluted to 4 wt% by adding distilled water. Finally, the dispersion was dried at 115°C overnight.

* To whom all correspondence should be sent:
E-mail: Ahmed.Afify@polito.it

The dried powder was treated at 800°C for 1 h with a heating ramp of 2°C/min. The powders were then manually grounded by means of an agate mortar and an agate pestle before the screen printing process.

Powder characterization

Particle size distribution was determined after powder calcination by means of a laser granulometer (Malvern 3600D) and after dispersion in ethanol and sonication for 10 min. X-ray diffraction patterns were collected on powders by means of an X'Pert High Score Philips Analytical Diffractometer, equipped with a Cu anticathode (λ Cu Kα anticathode= 0.154056 nm). Samples were scanned at a rate of 0.02°/ s in the range from 5° to 70° in 2θ after calcinations of the prepared powder. Finally, samples were chromium sputtered for FESEM (Field Emission Scanning Electron Microscopy, Zeiss Merlin) investigations.

Humidity sensor preparation and testing

The sensors were screen printed onto α- alumina substrates with platinum electrodes fired at 980°C for 20 min. (with a heating ramp of 2°C/min.) [25, 26]. Screen printing inks were made of the doped α-Fe_2O_3 powders and an organic vehicle (Terpenol), which acts as a temporary binder for the unfired film and confers the appropriate rheological properties to the paste.

After deposition the samples were dried in air at room temperature prior to being heat treated at 800°C, (with a heating ramp of 2°C/min.) for 1h. The humidity sensors were tested in a laboratory apparatus made of a thermostated chamber, operated at 25°C, in which the relative humidity (RH) could be varied between 0 and 96% [27].

The laboratory apparatus for testing the sensors was calibrated to ensure a constant air flow during the electrical measurements and RH was varied by steps, each one of 3 min. An external alternating voltage (V = 3.6 V at 1 kHz) was applied on each tested sensor, acting as a variable resistance of the electrical circuit described above. A 2000 series Keithley digital multimeter was used to measure the tension V_{DC} at the output of the circuit.

The sensor resistance was determined by a calibration curve drawn substituting the sensors, in the circuit, by known resistances. The sensor response (SR), expressed in %, was defined as the relative variation of the starting resistance, compared with the resistance measured under gas exposure (eq. 1):

$$SR(\%) = 100\frac{|R_0 - Rg|}{R_0} \quad \text{(eq. 1)}$$

Where R_0 and R_g are the starting (in the absence of the test gas) and the gas exposed measured resistances of the sensors, respectively.

RESULTS AND DISCUSSION

Materials characterization

Particle size distribution

Commercial α-Fe_2O_3 has a particle size distribution lower than 2 µm. Generally, doped metal ion–hematite samples thermally treated at 800°C for 1 h present a larger particle size distribution as shown in Table 1. This could be attributed to particle's agglomeration during the drying process. Moreover, the variation in size is due to their atomic radius.

The cumulative weight below 50% of the hematite doped metal ions particle size is less than 40 µm, means it could be passed through the opening of the screen-printing mesh. Sieving was performed for Sodium and Barium doped hematite to obtain a size less than 40 µm as shown in Fig.1.

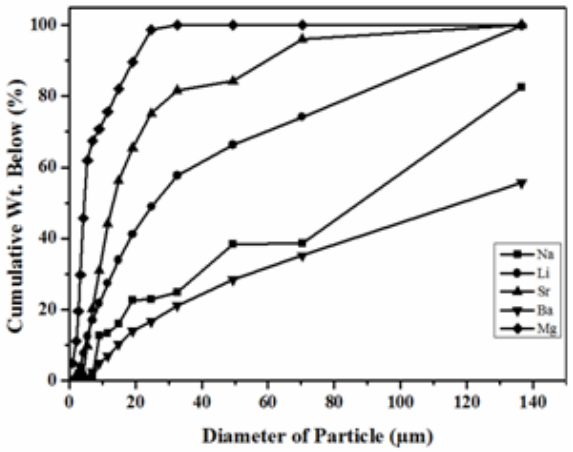

Fig. 1. Particle size distribution of metal ions doped onto hematite powders.

XRD measurements

For the sake of comparison with the metal-ions doped hematite, the XRD pattern of a commercial α-Fe_2O_3 (JCPDS card n°33-664) is shown in Fig. 2a. XRD patterns of the different doped α-Fe_2O_3 powders presented in Fig.2b, 2c, 3a, 3b showed well crystallized phases.

Sodium doped hematite was crystallized in $NaFeO_2$ form according to (JCPDS card n°1-74-1351), the structure of $NaFeO_2$ is a layer ordered rock salt type structure [27].

Table 1. Diameter of the doped metal ions hematite powders (µm)

Cumulative wt%	Na^+ (α-Fe_2O_3) [µm]	Li^+ (α-Fe_2O_3) [µm]	Sr^{2+} (α-Fe_2O_3) [µm]	Ba^{2+} (α-Fe_2O_3) [µm]	Mg^{2+} (α-Fe_2O_3) [µm]
10%	7.03	5.58	5.61	14.55	1.92
50%	91.13	25.36	13.19	122.62	4.7
90%	149.2	85.33	65.88	220.72	19.19

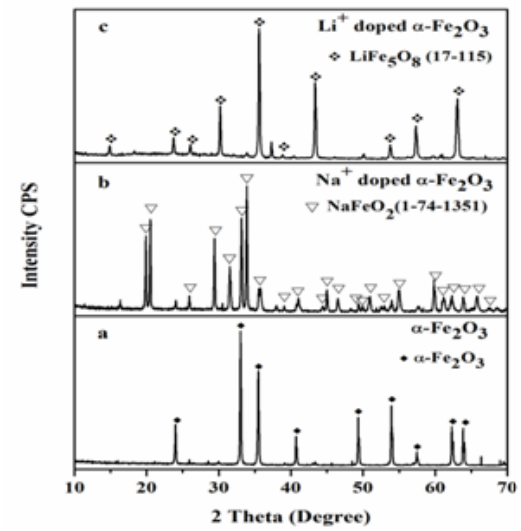

Fig. 2. XRD pattern of a) α-Fe_2O_3, b) sodium-doped hematite and c) lithium-doped hematite

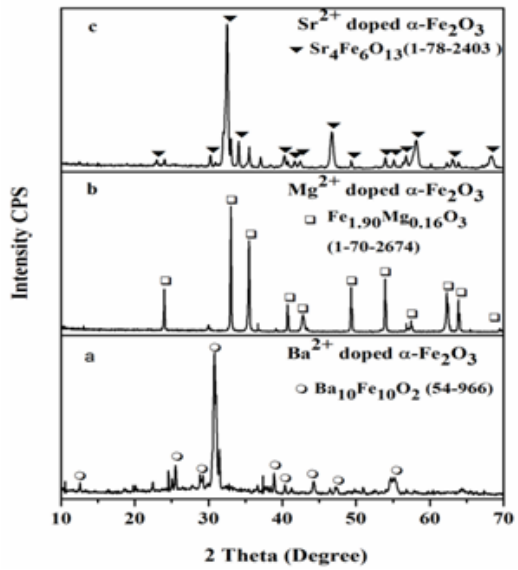

Fig.3. XRD pattern of a) barium-doped hematite, b) magnesium-doped hematite and c) strontium-doped hematite

$LiFe_5O_8$ (JCPDS card n°17-115) with a cubic spinel structure derived from lithium-doped hematite [28].

The $Sr_4Fe_6O_{13}$ phase obtained according to (JCPDS card n° 1-78-2403) from a strontium doped hematite sample, the phase formed when the powder calcined above 775°C which matches the thermally treated powder at 800°C [29].

$Ba_{10}Fe_{10}O_{28}$ (JCPDS cards n°54-966) and $Fe_{1.9}Mg_{0.16}O_3$ (JCPDS cards n°1-70-2674) are detected in barium and magnesium doped hematite, respectively.

FE-SEM observation and microanalysis

FESEM micrographs of unfired, fired at 800°C commercial hematite as well as Na^+ doped hematite heat treated at 800° are shown in Figs.4a, 4b and 4c respectively in order to distinguish the morphological difference between all of them.

According to the FESEM analysis, unfired hematite appears denser with less porosity than fired hematite (see Figs 4a, and 4b). Fired Na^+ doped hematite powder has the biggest grains size in comparison with the particles size of the fired and unfired hematite (see Figs 4a, 4b and 4c). This could be attributed to the diffusion of sodium ions into the crystalline hematite.

FESEM data also showed that the fired sodium doped hematite film is characterized by well distributed porosity, which makes this material appropriate as a gas sensor. Energy dispersive x-ray (EDX) analysis of sodium doped hematite showed that Na^+ and Fe^{+2} were well distributed in all the samples (see Table 2. and Fig. 5) which is in a good agreement with the XRD data for the $NaFeO_2$ phase.

Table 2. EDX of the fired Na-doped hematite sample at 800°C.

Metals	At%	Wt%
Na	8.42±1.2	3.65
Fe	91.58±3.2	96.35

Sensitivity towards relative humidity

Fig. 6 illustrates the sensors' response to RH. Among the different investigated samples, Na^+ doped hematite showed a significant response to RH at room temperature starting from 32% RH.

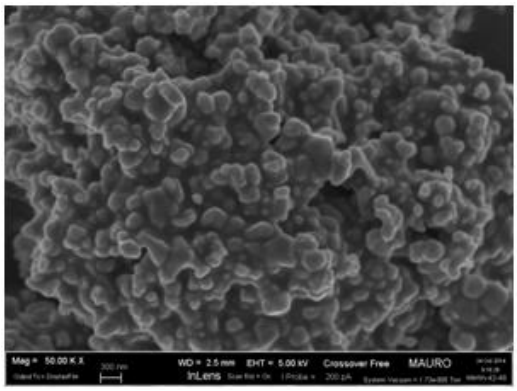

(a)

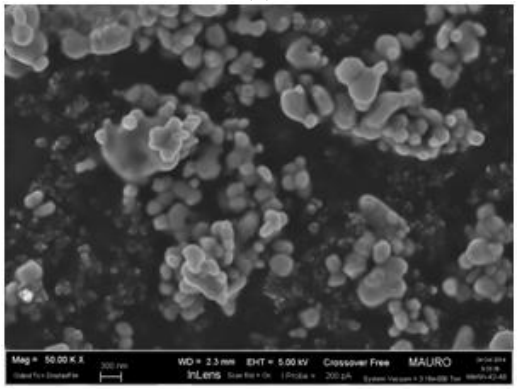

(b)

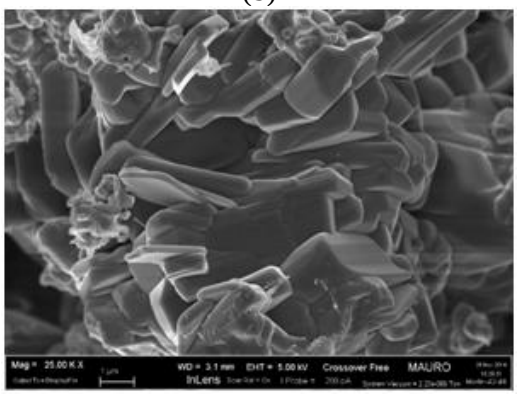

(c)

Fig. 4. FESEM micrographs of a) unfired hematite powder, b) hematite powder heat treated at 800°C for 1 h and c) Na^+ doped hematite heat treated at 800°C for 1 h.

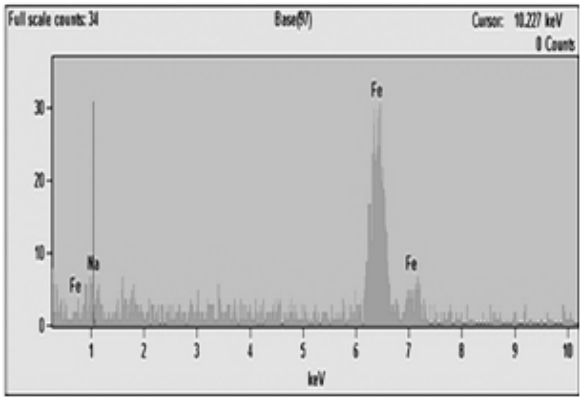

Fig. 5. EDX maps of fired sodium -doped hematite at 800°C

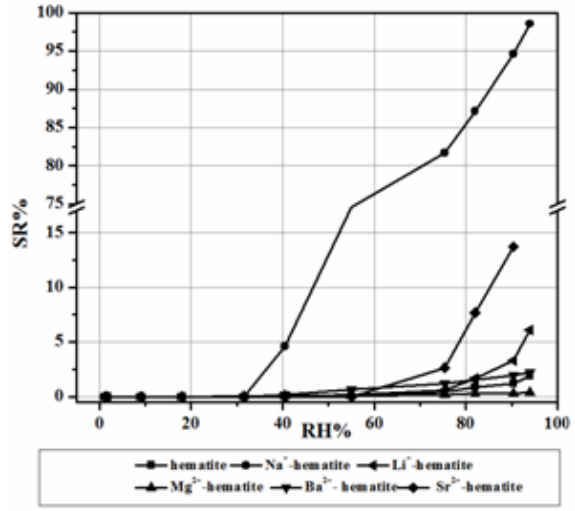

Fig. 6. Sensors response to relative humidity changes.

While the other metal ions doped hematite samples show a poor sensitivity to RH. Fig.7 shows the change in V_{DC} as a function of time for Na^+ doped hematite sensors. The response times (the time taken by a sensor to achieve 90% of the total resistance change in the case of gas adsorption) and the recovery times (the time necessary to reach 90% of the total resistance changes in the case of gas desorption) are reported in Table 3. These response and recovery times are quite fast.

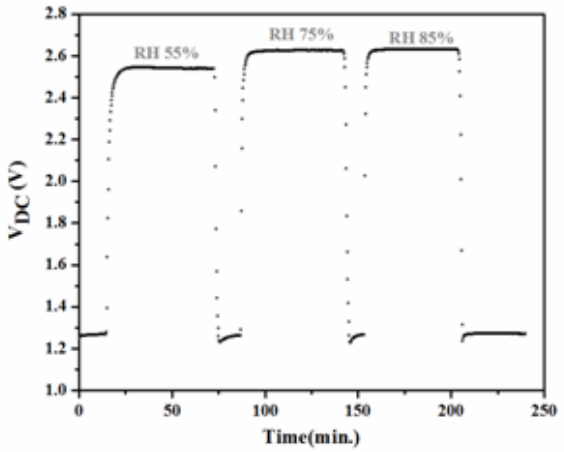

Fig. 7. Changes in V_{DC} as a function of RH changes at room temperature for Na^+ doped hematite sensor.

Table 3. Response and recovery time of the Na^+ doped hematite based sensor

Humidity change	0-55% RH	0-75% RH	0-85% RH
Response time (min.)	2.5	2.1	1.2
Humidity change	55-0% RH	75-0% RH	85-0% RH
Recovery time (min.)	1.0	2.5	2.5

CONCLUSION

A simple and low cost chemical method was used to synthesize hematite doped with different alkali and alkaline-earth metals. The screen printing technique was applied to realize humidity sensors from the prepared powders.

Doping of hematite with metal ions can create surface defects or oxygen vacancies that possess a high local charge density which increases the adsorption sites for water vapor. The investigated Li^{+}, Mg^{+2}, Ba^{+2}, and Sr^{+2} doped hematite based sensors exhibit a low sensitivity to RH.

While, Na^{+} doped hematite based sensors show a significant response towards RH and their response and recovery time were quiet fast. Further work should be devoted to improve the sensitivity of the sodium doped hematite in order to obtain novel RH sensors and to examine its sensitivity to other gases such as NO_x and H_2.

Acknowledgment: *This work was supported by the Erasmus-Mundus program (EMECW) through grants attributed to A. Afify (Action 2 WELCOME Project, Coordination Office: Politecnico di Torino, Turin, Italy) and M. Ataalla (Medastar Project, Coordination Office: Ovideo University, Madrid, Spain).*

REFERENCES

1. Q. Hao, L. Li, X. Yin, S. Liu, Q. Li, T. Wang, *Mat. Sci. Eng. B*, **176**, 600 (2011).
2. R. E. Newnham, *Br. Ceram. Trans.*, **98**, 251 (1999).
3. J. M. Tulliani, C. Baroni, L. Zavattaro, C. Grignani, *Sensors*, **13**, 12070 (2013).
4. K. Carr-Brion, Moisture Sensors in Process Control; Elsevier Applied Science Publishers: London, UK, 1986.
5. E. Traversa, *Sens. Actuators B*, **23**, 135 (1995).
6. T. Y. Kim, D. H. Lee, Y. C. Shim, J.U. Bu, S. T. Kim, *Sens. Actuators*, B, **9**, 221 (1992).
7. Y.C. Yek, T.Y. Tseng, *IEEE Trans. Compon. Hybrids Manufact. Technol.*, **12**, 259 (1989).
8. B. M. Kulwicki, *J. Am. Ceram. Soc.*, **74**, 697 (1991).
9. S. S. Nair, M. Mathews, P. A. Joy, S. D. Kulkarni, M. R. Anantharaman, *J. Mag. Mag. Mater.*, **283**, 344 (2004).
10. C. L. Zhu, Y. J. Chen, R. X. Wang, L. J. Wang, M. S. Cao, X. L. Shi, *Sens. Actuators B*, **140**, 185 (2009).
11. W. Weiss, D. Zscherpel, R. Schlögl, *Catal. Lett.*, **52**, 215 (1998).
12. B. C. Faust, M. R. Hoffmann, D.W. Bahnemann, *J. Phys. Chem.*, **93**, 6371(1989).
13. T. Ohmori, H. Takahashi, H. Mametsuka, E. Suzuki, *Phys. Chem. Chem. Phys.*, **2**, 3519 (2000).
14. A. K. Gupta, M. Gupta, *Biomaterials*, **26**, 3995 (2005).
15. E. Comini, V. Guidi, C. Frigeri, I. Riccò, G. Sberveglieri, *Sens. Actuators B*, **77**,16 (2001).
16. A. Y. Lipare, P. N. Vasambekar, A. S. Vaingankar, *J. Magn. Magn Mater*, **279**, 160 (2004).
17. E. L. Miller, D. Paluselli, B. Marsen, R. E. Rocheleau, *Thin Solid Films*, **466**, 307 (2004).
18. F. Zhou, S. Kotru, R. K. Pandey, *Thin Solid Films*, **408**, 33 (2002).
19. Y. S. Hu, A. Kleiman-Shwarsctein, A. J. Forman, D. Hazen, J. N. Park, E. W. McFarland, *Chem. Mater.*, **20**, 3803 (2008).
20. A. Duret, M. Grätzel, *J. Phys. Chem. B.*, **109**, 17184 (2005).
21. F. Le Formal, M. M. Grätzel, K. Sivula, *Adv. Funct. Mater.*, **20**, 1099 (2010).
22. L. Yuberto, M. Ocaña, A. Justo, L. Conttreras, A. R. González-Elipe, *J. Vac. Sci. Technol. A*, **18**, 2244 (2000).
23. B. J. Kim, E. T. Lee, G. E. Jang, *Thin Solid Films*, **341**, 79 (1999).
24. A. A. Tahir, K. G. Upul Wijayantha, S. Saremi-Yarahamadi, M. Mazhar, V. McKee, *Chem. Mater.*, **21**, 3763 (2009).
25. J. Savage, Handbook of Thick Film Technology, P. J. Holmes, R.G. Loasby Eds., Electrochemical Publications Ltd., Scotland, 1976, p. 51.
26. W. Qu, *Solid State Ionics*, **83**, 257 (1996).
27. M. Viret, D. Rubi, D. Colson, D. Lebeugle, A. Forget, P. Bonville, G. Dhalenne, R. Saint-Martin, G. Andre´, F. Ott, *Mater. Res. Bull.*, **47**, 2294 (2012).
28. F. O. Ernst, H. K. Kammler, A. Roessler, S. E. Pratsinis, W. J. Stark, J. Ufheil, P. Nova´k, *Mater. Chem. Phys.*, **101**, 372 (2007).
29. A. Fossdal, M.-A. Einarsrud, T. Grande, *J. Solid State Chem.*, **177**, 2933 (2004).

ИЗСЛЕДВАНЕ НА ЕФЕКТА НА ДОТИРАНЕ С МЕТАЛНИ ЙОНИ НА КРИСТАЛНИ ВЛАГОВИ СЕНЗОРИ НА ОСНОВАТА НА ХЕМАТИТ

А. Афифи[1], М. Атаалла[2], А. Хюсейн[1], М. Хасан[1], А. Мохамед[3], М. Миланова[4], Ж.М. Тюлиани[1]

[1]Политехнически университет, Факултет по наука и технологии, 10129 Торино, Италия
[2] Химикотехнологичен и металургичен университет, Факултет по материалознание 1758 София, България
[3] Институт по оптични технологии, Хелиополис, Кайро, Египет
[4] Институт по обща и неорганична химия, БАН

Постъпила на 24 март, 2015 г. коригирана на 26 октомври, 2015 г.

(Резюме)

Влаговите сензори намират широко приложение, както в индустриалното производство, така и за контрол на околната среда. Доказано е, че хематитът (α-Fe_2O_3), както недотиран, така и дотиран с различни метални йони показва забележителни свойства като влагов сензор. Целта на настоящето изследване е да се изучи ефекта на дотиране с метални йони (Li^+, Mg^{+2}, Ba^{+2}, Sr^{+2} и Na^+) на кристални влагови сензори на основата на хематит. Получените материали са охарактеризирани чрез рентенофазов анализ и сканираща електронна мискроскопия. Установено е, че Na^+-дотиран хематит показва показва висока чувствителност спрямо относителната влажност на въздуха при стайна температура.